Northumbria Research Link

www.northumbria.ac.uk/nrl

northumbria
UNIVERSITY NEWCASTLE

Impact of Link Parameters and Channel Correlation on the Performance of FSO Systems with Differential Signalling Technique

Mojtaba Mansour Abadi, Zabih Ghassemlooy, Stanislav Zvanovec, Manav R. Bhatnagar, Mohammad-Ali Khalighi, and Yongle Wu

Abstract—We investigate the effects of link parameters and the channel correlation coefficient on the detection threshold, Q-factor, and bit-error-rate (BER) of a free space optical system employing the differential signalling scheme. In systems employing differential signalling scheme, the mean value of the signal is used as the detection threshold level, provided that differential links are identical or highly correlated. However, in reality the underlying links are not essentially identical and have a low level of correlation. To show the significance of the link parameters as well as the correlation coefficient, we derive analytical relations describing the effect of weak turbulence and we determine the improvement of Q-factor with the channel correlation. Further, for the same signal-to-noise ratio, we demonstrate that a link with a higher extinction ratio offers improved performance. We also propose a closed-form expression of the system BER. We present experimental results showing improved Q-factor for the correlated channel case, compared to the uncorrelated channel.

The authors M. Mansour Abadi and Zabih Ghassemlooy are with Optical Communications Research Group, Faculty of Engineering and Environment, Northumbria University, Newcastle upon Tyne, NE1 8ST, U.K. (email: mojtaba.mansourabadi, z.ghassemlooy}@northumbria.ac.uk).

Stanislav Zvanovec is with the Department of Electromagnetic Field, Faculty of Electrical Engineering, Czech Technical University in Prague, 2 Technicka, 16627 Prague, Czech Republic (e-mail: xzvanove@fel.cvut.cz).

Manav R. Bhatnagar is with the Department of Electrical Engineering, Indian Institute of Technology Delhi, New Delhi, 110016, India (e-mail: manav@ee.iitd.ac.in).

Mohammad-Ali Khalighi is with École Centrale Marseille, Institut Fresnel, UMR CNRS 7249, Domaine Universitaire Saint-Jérôme, 13397 Marseille Cedex 20, France (e-mail: Ali.Khalighi@fresnel.fr).

Yongle Wu is with School of Electronic Engineering, Beijing University of Posts and Telecommunications, Beijing 100876, China (e-mail: wuyongle138@gmail.com).

Index Terms—Optical communication; free space optical (FSO) communication; differential signalling; on-off keying; channel estimation; atmospheric turbulence.

I. INTRODUCTION

The received signal in a free space optical (FSO) communication system is highly sensitive to the deterministic and random factors associated with the atmospheric channel, such as fog, smoke, low clouds, snow, rain, and turbulence [1-3]. Additionally, the pointing errors due to the building sway vibration and thermal expansion can further deteriorate the FSO link performance [4-6]. Whereas fog, smoke, rain, etc. expose a constant loss to the propagating optical signal, turbulence and pointing errors result in random fluctuation of the received signal. These fluctuations can be mitigated by adopting long inter-leaver spans combined with forward-error-correction [7]. Alternatively adaptive optics or spatial diversity can be employed to achieve a similar compensating effect [8].

To detect a non-return-to-zero on-off-keying (NRZ-OOK) modulated signal at the receiver (Rx), one can use a simple detection threshold scheme. However due to random fading within the channel, one should use an adjusted threshold level based on the fading strength. In [9] a maximum-likelihood sequence detection (MLSD) scheme was adopted for NRZ-OOK. It was shown that provided the temporal correlation of turbulence τ_0 is known, MLSD outperforms the maximum-likelihood symbol-by-symbol detection scheme. Given that $\tau_0 \cong 1 - 10$ ms MLSD suffers from high computational burden at the Rx, thus making the implementation of the Rx too complex. To reduce the computational complexity two suboptimal MLSD schemes based on the single-step Markov chain (SMC) model were derived in [10]. However, aforementioned schemes require perfect channel state information (CSI) at the Rx. Assuming that τ_0 is known, a pilot symbol is periodically added to the data frame in pilot-symbol assisted modulation (PSAM) to mitigate the effects of channel fading [11]. In PSAM the Rx still needs to know the fading correlation, thus the joint probability distribution of turbulence induced fading.

Meanwhile, the insertion of pilot symbols decreases the system throughput [11].

In the decision-feedback scheme, the detection is based on knowledge of previous decisions and an observation window over τ_0 [1]. The drawback of this scheme represents the dependency on the value of τ_0 and on the data pattern (i.e., stream bits 1 and 0) [1]. Fast multi-symbol detection which works based on block-wise decisions and a fast search algorithm was shown in [12]. The main drawback of this method is the trade-off between throughput and performance. A blind detection scheme for the case where there is no channel knowledge with the background-noise limited and a sub-optimum maximum-likelihood detection based Rxs was studied in [13] and [14], respectively. However, the performances of these schemes are rather poor for small observation windows. Recently an maximum-likelihood sequence Rx not requiring the knowledge of CSI, channel distribution, and transmitted power was proposed in [1] for usage under different channel conditions. However, the system is too complex to implement in commercial NRZ-OOK based systems. All mentioned detection methods need CSI either in instantaneous or statistical form; the detection threshold decision is either based on high computational process or using a pilot and training sequence where the former increases complexity and the latter reduces throughput.

In a single-ended signal, any signal variation introduced will be difficult to remove without using highly complex cancellation schemes. Therefore, single-ended signals are more prone to noise and electromagnetically coupled interference. On the other hand, in differential signalling an error introduced to a differential system path will be added to each of the two balanced signals equally. Since the return path is not a constant reference point, then the error will be cancelled. Consequently, differential signalling based schemes are less susceptible to noise and interference.

A differential signalling was adopted in [2, 15] to utilise a pre-fixed threshold level under various channel conditions (rain, turbulence, etc.). In order to reduce the impact of the background noise in [16] two laser wavelengths at the Tx and working in a differential mode at the Rx were investigated for OOK and pulse position modulation (PPM), where special signalling schemes were proposed to increase the transmission rate at the same time. Differential coherent detection is a simple way of achieving carrier synchronisation with phase shift keying (PSK). Provided there is no inter-symbol interference (ISI) it represents an alternative solution for systems, where error in signal is caused by the channel itself [17]. Compared to similar techniques e.g. the binary orthogonal differential signalling technique requires no signal processing as in 2-PPM. In the case of frequency-shift keying (FSK) implemented in the optical domain (i.e., using two distinct wavelengths), the system becomes too complex. However, in a single wavelength based FSK system with two orthogonal frequencies, the spacing between the frequencies is restricted by the data rate and the orthogonality criteria.

The differential signalling method is preferred to other detection optimization methods because of (i) no requirement for CSI or extensive computations at the Rx;

(ii) no need for the feedback signal to adjust the threshold level; (iii) no effect on the system throughput, since no pilot or training sequence are used; (iv) mitigation of the background noise at the Rx [16]; (v) the atmospheric channel conditions such as: fog, smoke [2]; (vi), turbulence [15], and pointing errors [18]; and (vii) the use of a common aperture for both FSO links, since the method benefits from high correlation between two FSO channels. Note, the differential signalling method applied for correlated channels was investigated in [15] for the identical link however with no results in terms of the bit-error-rate (BER) performance and the **Q**-factor. Besides, to the best of authors' knowledge no research works have been reported on the effect of channel correlation based on the differential signalling technique.

In this paper we generalise the scheme proposed in [2] and [15], and investigate the effect of correlation coefficient and link parameters on the threshold level as well as the Q-factor. Besides we demonstrate that the differential signalling method improves the Q-factor of the received signal, and present a method to analytically determine the BER. Finally, experimental work is presented as a proof of concept to show the improvement in the Q-factor for the correlated channels. Note that in a previous work, we investigated the concept of differential signalling in correlated channels for the specific case of quasi-identical links, where the link performance was evaluated by considering the detection threshold for the case of OOK signalling [15]. In this paper we generalise the idea of differential signalling for the cases where the links are different and, furthermore, the link performance is evaluated in terms of the Q-factor and BER.

The paper is organized as follows. Section II describes the proposed differential signalling model by means of deriving general mathematical expressions. Section III is devoted to deriving the BER expression. Section IV presents numerical analyses to investigate the effect of correlation coefficient and link parameters on the threshold level and Q-factor. We also discuss the effect of correlation coefficient on BER. In section V the experiment is described to demonstrate the effect of correlation coefficient on the Q-factor. Section VI concludes the paper.

II. DIFFERENTIAL SIGNALLING MODELLING

The proposed system block diagram is depicted in Fig. 1. The NRZ-OOK input signal $S \in \{0,1\}$ and its inverted version $\bar{S}$ are used to drive the optical sources (OSs) interpreted as x_1 and x_2, respectively. Knowing that superscripts high and low denote corresponding high and low levels of the electrical signal, respectively then we have:

$$x_i = \begin{cases} V_i^{high} & \text{if } i = 1 \text{ bit 1, otherwise bit 0} \\ \left(V_i^{high} + V_i^{low}\right)/2 & \text{Threshold Level} \\ V_i^{low} & \text{if } i = 1 \text{ bit 0, otherwise bit 1} \end{cases} . \quad (1)$$

One can regenerate information bits by comparing the signal to the corresponding threshold level value given in (1). x_1 and x_2 are used for intensity modulation of two OS at wavelengths of λ_1 and λ_2. The light outputs of OS are combined using a beam combiner prior to being transmitted over the FSO channel of length L.
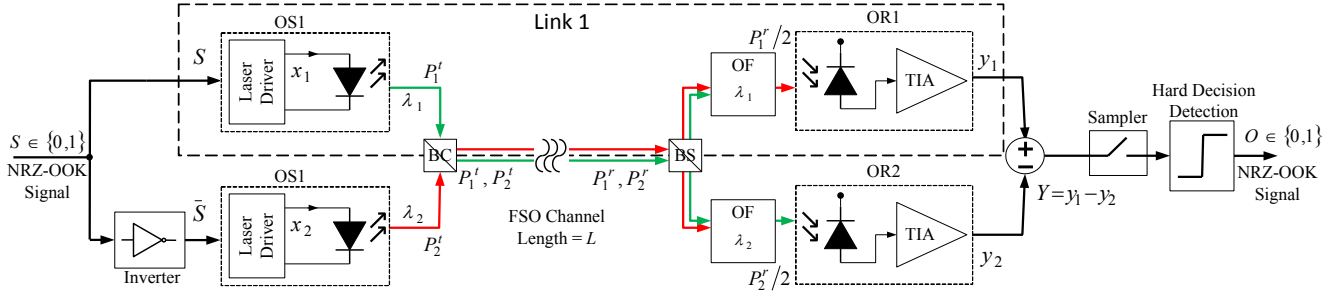
Fig. 1. Differential signalling system schematic block diagram. OS, BC, BS, OF, and OR are optical source, beam combiner, beam splittetr, optical filter, and optical Rx, respectively.

The received optical signal $P_i^r = h_i P_i^t$, where h_i and P_i^t are the channel coefficient and the transmit power, respectively. h_i represents a combined effect of the geometrical attenuation, atmospheric loss (due to fog, smoke, low clouds, snow, and rain), pointing errors and atmospheric turbulence. In this paper we only consider turbulence, and without loss of generality other effects are not taken into account. The received optical signal is passed through a 50/50 beam splitter and optical filters with the centre wavelengths of λ_1 and λ_2, prior to being collected by two identical photodetectors (PDs). The generated photocurrents are amplified by transimpedance amplifiers. The outputs of optical receivers (ORs) are given by:

$$y_i = n_i + \begin{cases} h_i G_i \Re_i \frac{\varepsilon_i P_i^{avg}}{1+\varepsilon_i} & \text{if } i = 1 \text{ bit } 1, \text{otherwise bit } 0 \\ \frac{1}{2} h_i G_i \Re_i P_i^{avg} & \text{Threshold Level} \\ h_i G_i \Re_i \frac{P_i^{avg}}{1+\varepsilon_i} & \text{if } i = 1 \text{ bit } 0, \text{otherwise bit } 1 \end{cases} , (2)$$

where $\Re_i$ is the PD responsivity, G_i is gain of transimpedance amplifiers, ε_i is extinction ratio, and n_i is the additive white Gaussian noise (AWGN) with the mean value of zero and variance of $\sigma_{n,i}^2$. Note that P_i^{high} and P_i^{low} refers to low and high power levels, therefore $P_i^{avg} = \left(P_i^{high} + P_i^{low}\right)/2$ and $\varepsilon_i = P_i^{high}/P_i^{low}$.

Considering a single-input single-output (SISO) FSO link (see link 1 in Fig. 1), we define the average value Mean($\cdot$) and the variance of the received electrical signal Var($\cdot$). as [19]:

$$\text{Mean}(y_1) = \begin{cases} \frac{\varepsilon_1 \Phi_1}{(1+\varepsilon_1)} & \text{bit } 1 \\ \Phi_1 & \text{Threshold}, \\ \frac{\Phi_1}{(1+\varepsilon_1)} & \text{bit } 0 \end{cases} (3a)$$

$$\text{Var}(y_1) = \sigma_{n,1}^2 + \left[\exp\left(4\sigma_{h,1}^2\right) - 1\right] \times \begin{cases} \left(\frac{2\varepsilon_1 \Phi_1}{(1+\varepsilon_1)}\right)^2 & \text{bit } 1 \\ (\Phi_1)^2 & \text{Threshold}, \\ \left(\frac{2\Phi_1}{(1+\varepsilon_1)}\right)^2 & \text{bit } 0 \end{cases} (3b)$$

where $\Phi_i = G_i \Re_i P_i^{avg}$. Since we assume a weak turbulence regime, h_i has log-normal distribution with the mean and variance parameters of $\mu_{h,i}$ and $\sigma_{h,i}^2$, respectively [19] where $\mu_{h,i} = -\sigma_{h,i}^2$[20]. Also from the literature [19], we have adopted
$\text{Mean}(h_i) = \exp\left(2\mu_{h,i} + 2\sigma_{h,i}^2\right)$ and $\text{Var}(h_i) = \left(\exp\left(4\sigma_{h,i}^2\right) - 1\right) \times$

$\exp\left(4\mu_{h,i} + 4\sigma_{h,i}^2\right)$ in order to obtain (3).

The expression in (3a) shows that the average of threshold level depends on $\sigma_{h,1}^2$. Besides based on (3b) the threshold level fluctuates with a given order. The expressions in (3) show that a constant threshold level is not appropriate in a SISO system under the turbulence effect. As mentioned before, several complex methods have been proposed to compensate the random aspect of threshold level in a turbulence channel. However, we will show that it is possible to remove the random behaviour of the threshold level for specific link conditions to maintain a fixed threshold level under various turbulence conditions.

Now considering the differential signalling scheme, the combined output $Y = y_1 - y_2$ is sampled at the centre of bit duration and a threshold detector is used to regenerate the data signal by comparing the sampled signal with a fixed threshold. The Mean(Y) and Var(Y) are given as:
$\text{Mean}(Y) =$

$$\begin{cases} \frac{\varepsilon_1 \Phi_1}{(1+\varepsilon_1)}\text{Mean}(h_1) - \frac{\Phi_2}{(1+\varepsilon_2)}\text{Mean}(h_2) & \text{bit } 1 \\ \frac{\Phi_1}{2}\text{Mean}(h_1) - \frac{\Phi_2}{2}\text{Mean}(h_1) & \text{Threshold Level} \\ \frac{\Phi_1}{(1+\varepsilon_1)}\text{Mean}(h_1) - \frac{\varepsilon_2 \Phi_2}{(1+\varepsilon_2)}\text{Mean}(h_2) & \text{bit } 0 \end{cases} (4a)$$

$\rho_{1,2}$ in (4b) is the correlation coefficient between the two signals. See next page for (4b). Provided that there are two propagating laser beams very close to each other they will experience the same turbulence strengths $\sigma_{h,1}^2 \approx \sigma_{h,2}^2$, thus we have:

$$\text{Mean}(Y) = \begin{cases} \frac{2\varepsilon_1 \Phi_1}{(1+\varepsilon_1)} - \frac{2\Phi_2}{(1+\varepsilon_2)} & \text{bit } 1 \\ \Phi_1 - \Phi_2 & \text{Threshold} \\ \frac{2\Phi_1}{(1+\varepsilon_1)} - \frac{2\varepsilon_2 \Phi_2}{(1+\varepsilon_2)} & \text{bit } 0 \end{cases} (5a)$$

See next page for (5b). By setting $\Phi_1 = \Phi_2$ or equivalently $G_1 \Re_1 P_1^{avg} = G_2 \Re_2 P_2^{avg}$ in (5a), the average of the threshold level is fixed to ~0 regardless of the turbulence regime. On the other hand, the variance of the threshold level under the same condition will be:
$$\text{Var}(Y_{TL}) = 2\left[\exp\left(4\sigma_{h,1}^2\right) - 1\right](\Phi_1)^2\left(1 - \rho_{1,2}\right) + \sigma_{n,1}^2 + \sigma_{n,2}^2, (6)$$

where Y_{TL} denotes the threshold level. To recover the transmit bit stream the pre-fixed threshold level should be set to 0, as in [2]. However in [2] the authors did not consider (6) and because of turbulence the actual signal threshold level fluctuates with the order given in (6). However for $\rho_{1,2} = 1$ (i.e., fully correlated beams/channels), $\text{Var}(Y_{TL}) = \sigma_{n,1}^2 + \sigma_{n,2}$ (i.e.,   no   turbulence   induced

$$\text{Var}(Y) = \sigma_{n,1}^2 + \sigma_{n,2}^2 +$$

$$\begin{cases} \left(\frac{\varepsilon_1 \Phi_1}{(1+\varepsilon_1)}\right)^2 \text{Var}(h_1) + \left(\frac{\Phi_2}{(1+\varepsilon_2)}\right)^2 \text{Var}(h_2) - 2\rho_{1,2}\frac{\varepsilon_1 \Phi_1 \Phi_2}{(1+\varepsilon_1)(1+\varepsilon_2)}\sqrt{\text{Var}(h_1)}\sqrt{\text{Var}(h_2)} & \text{bit 1} \\ \frac{(\Phi_1)^2}{4}\text{Var}(h_1) + \frac{(\Phi_2)^2}{4}\text{Var}(h_1) - \rho_{1,2}\frac{\Phi_1 \Phi_2}{2}\sqrt{\text{Var}(h_1)}\sqrt{\text{Var}(h_2)} & \text{Threshold Level.} \\ \left(\frac{\Phi_1}{(1+\varepsilon_1)}\right)^2 \text{Var}(h_1) + \left(\frac{\varepsilon_2 \Phi_2}{(1+\varepsilon_2)}\right)^2 \text{Var}(h_2) - 2\rho_{1,2}\frac{\varepsilon_2 \Phi_1 \Phi_2}{(1+\varepsilon_1)(1+\varepsilon_2)}\sqrt{\text{Var}(h_1)}\sqrt{\text{Var}(h_2)} & \text{bit 0} \end{cases} \quad (4b)$$

$$\text{Var}(Y) = \sigma_{n,1}^2 + \sigma_{n,2}^2 + [\exp(4\sigma_{h,1}^2)-1] \times \begin{cases} \left(\frac{2\varepsilon_1 \Phi_1}{(1+\varepsilon_1)}\right)^2 + \left(\frac{2\Phi_2}{(1+\varepsilon_2)}\right)^2 - 2\rho_{1,2}\frac{4\varepsilon_1 \Phi_1 \Phi_2}{(1+\varepsilon_1)(1+\varepsilon_2)} & \text{bit 1} \\ (\Phi_1)^2 + (\Phi_2)^2 - 2\rho_{1,2}\Phi_1\Phi_2 & \text{Threshold.} \\ \left(\frac{2\Phi_1}{(1+\varepsilon_1)}\right)^2 + \left(\frac{2\varepsilon_2 \Phi_2}{(1+\varepsilon_2)}\right)^2 - 2\rho_{1,2}\frac{4\varepsilon_2 \Phi_1 \Phi_2}{(1+\varepsilon_1)(1+\varepsilon_2)} & \text{bit 0} \end{cases} \quad (5b)$$

fluctuations). According to [21] for the weak turbulence regime, $\rho_{1,2}$ can be expressed in terms of the transversal distance between the Rx apertures d_r and the spatial coherence radius ρ_0. Here d_r is referred to the distance between the propagation axes of beams. The correlation coefficient between channels takes the form of [21]:

$$\rho_{1,2} = \exp\left[-\left(\frac{d_r}{\rho_0}\right)^{5/3}\right], \quad (7)$$

where for a plane wave propagation model ρ_0 is readily calculated as [22]:

$$\rho_0 = \left(1.455\left(\frac{2\pi}{\lambda}\right)^2 C_n^2 L\right)^{-3/5}, \quad (8)$$

where C_n^2 is the refractive index structure coefficient (unit of m$^{-2/3}$), which gives an indication of the turbulence strength [20]. From (7) for $d_r \to 0$ we have $\rho_{1,2} \to 1$. We pick the criteria of $d_r/\rho_0 \le 0.26$ for $\rho_{1,2} \ge 0.9$. Therefore, by adopting the differential signalling detection method and setting the spacing between the two propagating optical beams to zero, the effect of turbulence on the threshold level at the Rx can be significantly reduced. The simplicity of differential signalling is because of no requirement for the knowledge of CSI and the temporal correlation of turbulence, as well as reduced computational burden at the Rx and/or the need for buffering the received signal.

From (5) one can formulate the average and the variance of low and high levels of the combined signal $Y_{\text{bit }0}$ and $Y_{\text{bit }1}$, respectively as:

$$\text{Mean}(Y_{\text{bit }0}) = 2\Phi_1\left[\frac{1}{(1+\varepsilon_1)} - \frac{\varepsilon_2}{(1+\varepsilon_2)}\right], \quad (9a)$$

$$\text{Mean}(Y_{\text{bit }1}) = 2\Phi_1\left[\frac{\varepsilon_1}{(1+\varepsilon_1)} - \frac{1}{(1+\varepsilon_2)}\right], \quad (9b)$$

$$\text{Var}(Y_{\text{bit }0}) = 4[\exp(4\sigma_{h,1}^2)-1](\Phi_1)^2\left[\left(\frac{1}{(1+\varepsilon_1)}\right)^2 + \left(\frac{\varepsilon_2}{(1+\varepsilon_2)}\right)^2 - 2\rho_{1,2}\frac{\varepsilon_2}{(1+\varepsilon_1)(1+\varepsilon_2)}\right] + \sigma_{n,1}^2 + \sigma_{n,2}^2, \quad (9c)$$

$$\text{Var}(Y_{\text{bit }1}) = 4[\exp(4\sigma_{h,1}^2)-1](\Phi_1)^2\left[\left(\frac{\varepsilon_1}{(1+\varepsilon_1)}\right)^2 + \left(\frac{1}{(1+\varepsilon_2)}\right)^2 - 2\rho_{1,2}\frac{\varepsilon_1}{(1+\varepsilon_1)(1+\varepsilon_2)}\right] + \sigma_{n,1}^2 + \sigma_{n,2}^2. \quad (9d)$$

Using (9), Q-factor parameter can be determined to study the effect of channel characteristics on the received signal in differential signalling based FSO system as [23]:

$$Q = \frac{|\text{Mean}(Y_{\text{bit }1}) - \text{Mean}(Y_{\text{bit }0})|}{\sqrt{\text{Var}(Y_{\text{bit }1})} + \sqrt{\text{Var}(Y_{\text{bit }0})}}. \quad (10)$$

III. BER EXPRESSION

To derive a closed-form expression for the BER, we consider the simple case where both links have the same characteristics. Thus the received signal following the subtraction is given by:

$$Y = S\eta I_1 - \bar{S}\eta I_2 + n, \quad (11)$$

where η is the overall optical-to-electrical conversion coefficient, I_i ($i = 1,2$) represent the received optical intensities from each channel, and $n = n_1 - n_2$. The fading of this intensity is given as $I = I_0\exp(2X)$, where I_0 denotes the average signal intensity without turbulence and X is a distributed normal random variable with mean μ and variance σ^2 [20]. Under a weak turbulence regime, I has the lognormal PDF [20]:

$$f_I(I) = \frac{1}{2I}\frac{1}{\sqrt{2\pi\sigma^2}}\exp\left(-\frac{(\ln(I/I_0)-2\mu)^2}{8\sigma^2}\right). \quad (12)$$

Since both links are identical, $\text{E}[I_1] = \text{E}[I_2] = I_0$. In an electrical term, S is represented by two distinct signal levels of v_{low} and v_{high} corresponding to bits 0 and 1, respectively. For $\bar{S}$ the bits 0 and 1 are recognised as v_{high} and v_{low}. This means that for the link 1 in Fig. 1 the electrical received signals corresponding to bits 0 and 1 are $v_{\text{low}}\eta I_0 + n$ and $v_{\text{high}}\eta I_0 + n$, respectively. The received differential signalling signals for bits 0 and 1 are $(v_{\text{low}} - v_{\text{high}})\eta I_0 + n$ and $(v_{\text{high}} - v_{\text{low}})\eta I_0 + n$, respectively. The difference between these two bits is twice that of a single link, so without the loss of generality we replace levels of bits 0 and 1 with $2v_{\text{low}}\eta I_0 + n$ and $2v_{\text{high}}\eta I_0 + n$ and rewrite (11) by:

$$Y = S\eta I_{\text{DS}} + n_1 - n_2, \quad (13)$$

where we substitute the subtraction of received intensities by I_{DS}. The summation of two lognormal variables is usually approximated by lognormal variable [24, 25]. Here, we make the same assumption for I_{DS} (the validity of our assumption will be further discussed in section IV.D) that $I_{DS} = I_0\exp(2X_{DS})$, where X_{DS} is a normal random variable with mean μ_{DS} and variance σ_{DS}^2. We will use the same procedure as in Wilkinson's method [24], to estimate the required parameters of I_{DS}. To further normalize I_{DS} we set $\mu_{\text{DS}} = -\sigma_{\text{DS}}^2$, where σ_{DS}^2 is given by [19]:

$$\sigma_{\text{DS}}^2 = \ln\left(1 + \frac{\text{Var}[I_{DS}]}{I_0^2}\right), \quad (14)$$

where $\text{Var}(I_{DS})$ is given by [15]:

$$\text{Var}(I_{DS}) = \text{Var}(I_1) + \text{Var}(I_2) - 2\rho_{1,2}\sqrt{\text{Var}(I_1)\text{Var}(I_2)}. \quad (15)$$

Once σ_{DS}^2 is achieved it is possible to specify the PDF of a

differential signalling based FSO system by means of (12). Having obtained the PDF, the average BER of the link is defined as [26]:

$$\text{BER} = \int_0^\infty f_I(I)\mathbf{Q}\left(\frac{\eta I}{\sqrt{2N_0}}\right)dI, \tag{16}$$

where $\mathbf{Q}(x) = \int_x^{+\infty}\exp(-t^2/2)\,dt$ and N_0 is the AWGN power spectral density., For the closed-form expression of (16) please refer to [26].

IV. NUMERICAL ANALYSIS

A. Proof of Concept

To show the strength of the turbulence, Rytov variance σ_R^2 can be used [8]. For a weak turbulence regime $\sigma_R^2 < 1$ [27]. In the case of a plane wave propagation through a turbulence channel we have [8]:

$$\sigma_{h,i}^2 = \sigma_R^2/4 = 0.3075(2\pi/\lambda)^{7/6}C_n^2 L^{11/6}. \tag{17}$$

In this analysis, we used the wavelengths of 830 and 850 nm and a transmission link span of 1 km. To calculate Mean(Y_{TL}) and $\sqrt{\text{Var}(Y_{TL})}$ of SISO and differential signalling links (3) and (5) were used, respectively, whereas (10) was used to determine the Q-factor. In the performed analysis, the given value of SNR denotes the electrical SNR of the signal prior to the sampler module as shown in Fig. 1.

From (3) and (5), it is deduced that threshold level is dependent on ε_i. To confirm it, we used Monte-Carlo simulation for both SISO and differential signalling systems for $\varepsilon_i = 5$ and 10 with $\Phi_1 = \Phi_2 = 5.7$ mV, $\Phi_{SISO} = 8.1$ mV, $\rho_{1,2} = 1$, and $\sigma_R^2 = 0.5$. The obtained results are summarized in Table I. Considering the predicted and simulated results, we can see that the proposed theory predicts the system behaviour accurately. Besides in agreement with (3) and (5), for the same link condition but different values of ε_i, Mean(Y_{TL}) and $\sqrt{\text{Var}(Y_{TL})}$ are the same.

As discussed earlier when $\Phi_1 = \Phi_2$ and $\rho_{1,2} = 1$, for various turbulence conditions, Mean(Y_{TL}) ≈ 0 and Var(Y_{TL}) = $\sigma_{n,1}^2 + \sigma_{n,2}^2$. To show this, we performed another set of analyses for a range of turbulence strength from almost a clear channel $\sigma_R^2 \approx 0$ to $\sigma_R^2 = 1$ and $\rho_{1,2} = 1$. As we showed the value of ε_i does not affect Mean(Y_{TL}) and $\sqrt{\text{Var}(Y_{TL})}$, therefore for our simulation we set $\varepsilon_i = 10$ and by changing Φ_i we changed SNR.

Figures 2(a,b) show Mean(Y_{TL}) and $\sqrt{\text{Var}(Y_{TL})}$, respectively as a function of σ_R^2 for $\varepsilon_i = 10$ and SNR values of 10, 12, 14 dB. As can be seen for the differential signalling link plots in both figures are almost flat, whereas for the SISO link the Mean(Y_{TL}) is reduced by a small amount and $\sqrt{\text{Var}(Y_{TL})}$ exponentially increases with the turbulence strength. From Figs. 2(a,b) we can see that the theory can predict Mean(Y_{TL}) for both SISO and differential signalling cases. For $\sqrt{\text{Var}(Y_{TL})}$, there is a slight deviation between the theory and simulation, however both show the same behaviour. As predicted from (3) Mean(Y_{TL}) and $\sqrt{\text{Var}(Y_{TL})}$ of the SISO link change with the turbulence strength. $\sqrt{\text{Var}(Y_{TL})}$ of the SISO link is almost equal to $\sigma_{n,SISO} = 1.32$ mV for the clear channel condition (i.e., $\sigma_R^2 \approx 0$) and increases for higher values of σ_R^2, which agrees with (3b). Besides, different values of SNR result in a range of Mean(Y_{TL}) and $\sqrt{\text{Var}(Y_{TL})}$ for the SISO

TABLE I
THE SUMMARY OF THEORETICAL ANALYSIS AND SIMULATION OF SINGLE-INPUT SINGLE-OUTPUT (SISO) AND DIFFERENTIAL SIGNALLING (DS) LINKS FOR $\Phi_1 = \Phi_2 = 5.7$ MV, $\Phi_{SISO} = 8.1$ MV, $\rho_{1,2} = 1$, AND $\sigma_R^2 = 0.5$. ε, $\rho_{1,2}$, AND σ_R^2 DENOTE EXTINCTION RATIO, CORRELATION COEFFICIENT, AND RYTOV VARIANCE, RESPECTIVELY.

ε	SNR (dB)	Link	Mean (mV)[a]	$\sqrt{\text{Var}}$ (mV)[b]
5	12.2	SISO	7.1, 8.1	3.0, 3.3
		DS	0.0, 0.0	1.9, 2.0
10	14	SISO	7.1, 8.1	3.0, 3.4
		DS	0.0, 0.0	1.9, 1.8

[a], [b] For each case there is a pair of numbers with the 1st and 2nd numbers denoting predicted and simulated results.

link. In this analysis ε_i was fixed and then the SNR was changed by setting $\Phi_i = G_i \Re_i P_i^{avg}$. Thus the gain of transimpedance amplifiers, PD responsivity, and the laser beam output power can change the required threshold level whereas ε_i has no effect at all. On the other hand for the differential signalling link, Mean(Y_{TL}) remains fixed for different turbulence conditions and a range of SNR. This is expected since from (5a) for links having the same parameters (i.e., $\Phi_1 = \Phi_2$) and beams undergoing the same turbulence effect, the required threshold level at the Rx is zero. $\sqrt{\text{Var}(Y_{TL})}$ of the differential signalling link is also fixed for a range of SNR and turbulence regimes. From (5b) we have $\sqrt{\text{Var}(Y_{TL})} \approx (\sigma_{n,1}^2 + \sigma_{n,2}^2)^{1/2} = 1.9$ mV, which agrees well with the simulation results shown in Fig. 2(b).

Next, we compare the Q-factor against σ_R^2 for SISO and differential signalling links under different conditions. From (3), (5), and (10), we see that contrary to Mean(Y_{TL}) and $\sqrt{\text{Var}(Y_{TL})}$, the Q-factor also depends on ε_i. For a clear channel condition, $\text{Q}^2 \approx 10^{SNR/10}$, which reduces as σ_R^2 increases. By comparing Figs. 2(c,d), we see that changing ε_i from 5 to 10 has no effect on the Q-factor of the differential signalling link with $\rho_{1,2} = 1$. However the SISO link exhibits a lower Q-factor for $\varepsilon = 5$ under turbulent conditions.

B. Wavelength Separation

It is important to note that (17) gives different results for λ_1 and λ_2, which leads to $\sigma_{h,1}^2 \neq \sigma_{h,2}^2$. Therefore, the simplified expressions in (5) are no longer valid. Also note that, ρ_0 in (8) is a function of λ therefore it is essential to define the limitation on the wavelength difference $\Delta\lambda$, which still validates the use of (7), (8), and (17). Taking the derivatives of $\sigma_{h,i}^2$, $\rho_{1,2}$, and ρ_0 with respect to λ_i, and following a series of mathematical simplification, we have:

$$\Delta\sigma_{h,i}^2 = \frac{7}{6}\sigma_{h,i}^2\frac{\Delta\lambda}{\lambda_0}, \tag{18a}$$

$$\Delta\rho_0 = \frac{6}{5}\rho_0\frac{\Delta\lambda}{\lambda_0}, \tag{18b}$$

$$\Delta\rho_{1,2} = -2\rho_{1,2}\ln(\rho_{1,2})\frac{\Delta\lambda}{\lambda_0}, \tag{18c}$$

where $\lambda_0 = (\lambda_1 + \lambda_2)/2$ and $\Delta\lambda = |\lambda_1 - \lambda_2|$. Considering the rule of thumb, that a 10% tolerance relative to the absolute value is acceptable, from (18a) and (18b) the criteria of $\Delta\lambda/\lambda_0 < \frac{5}{60}$ is extracted. Under this criteria, which is not
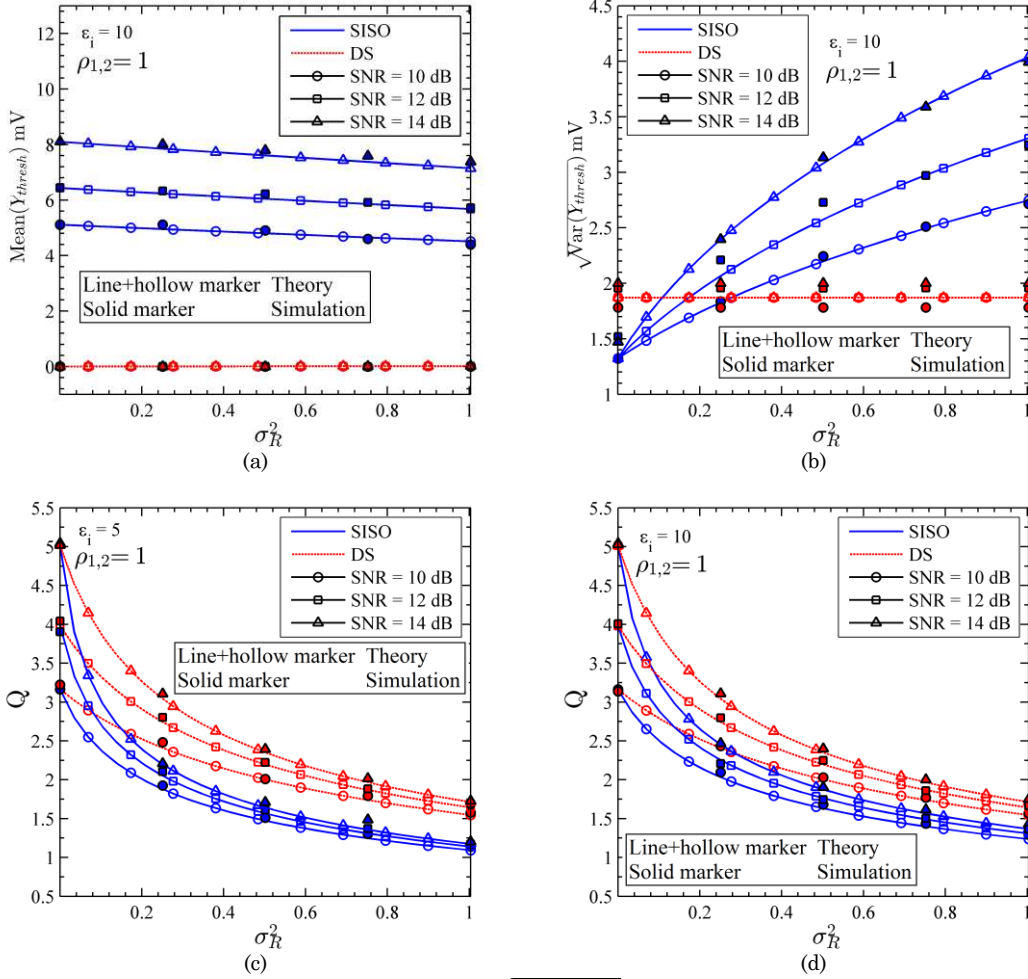
Fig. 2. Theory and simulation results for: (a) Mean(Y_{thresh}), (b) $\sqrt{\text{Var}(Y_{thresh})}$ for $\varepsilon_i = 10$ and a range of SNR, (c) and (d) the Q-factor for $\varepsilon_i = 5$ and $\varepsilon_i = 10$, respectively and various SNR. The calculation is done over a range of turbulence strength (i.e., σ_R^2) while $\rho_{1,2} = 1$. SISO and DS refer to single-input single-output and differential signalling, respectively, while ε_i and $\rho_{1,2}$ denote extinction ratio and correlation coefficient, respectively.

dependent on the FSO channel (i.e., C_n^2 and d_r), both (8) and (17) give approximate results for λ_1 and λ_2 with 10% of relative deviation. It can be easily shown that assuming the same rule of thumb of $\Delta\rho_{1,2}/\rho_{1,2} < 0.1$ the criteria based on (18c) will be given as:

$$\frac{\Delta\lambda}{\lambda_0} = \frac{1}{20}\left(\frac{d_r}{\rho_0}\right)^{-5/3}, \tag{19}$$

Figure 3 depicts a plot of $\Delta\lambda/\lambda_0$ against d_r/ρ_0, showing a characteristic, which is independent of the wavelength. For $d_r/\rho_0 \rightarrow 0$ the range applicable λ_1 and λ_2 broadens (i.e., $\Delta\lambda/\lambda_0 \rightarrow \infty$) whereas for $0 < d_r/\rho_0 < 0.26$ the range is reduced (i.e. $\Delta\lambda/\lambda_0 > 0.47$). Therefore, there is a trade-off between selecting the operating wavelengths and how spatially closer the propagating optical beams can be.

C. Correlation Coefficient

For the differential signalling link the two conditions of $\Phi_1 = \Phi_2$ and $\rho_{1,2} \rightarrow 1$ are outlined for the ideal scenario. Next we consider more realistic values for Φ_i and $\rho_{1,2}$ and compare Mean(Y_{TL}), $\sqrt{\text{Var}(Y_{\text{TL}})}$ and the Q-factor for both SISO and differential signalling links - see Fig. 4 for the SNR of 12 dB, ε of 5, 10, and 20 and $\sigma_R^2 \approx 0.5$. Note that the

value of Φ_i was decided based on the required SNR and a given value of ε. E.g., for $\varepsilon = 5$, $\Phi_{\text{SISO}} = 7.9$ mV for the SISO link, whereas for the differential signalling link $\Phi_1 = 6.3$ mV

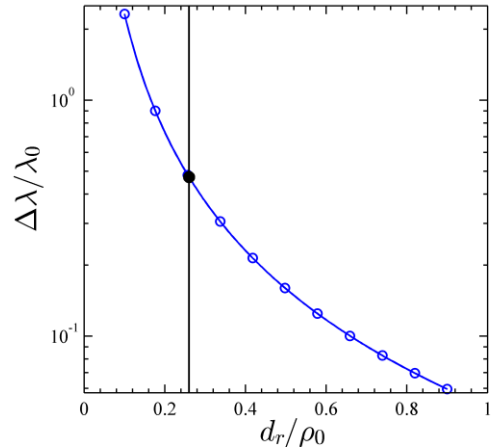Fig. 3. $\Delta\lambda/\lambda_0$ plotted with respect to d_r/ρ_0. The vertical line shows the criteria of $d_r/\rho_0 = 0.26$ and the solid dot marker denotes $\Delta\lambda/\lambda_0 = 0.47$. The graph is plotted based on (19).
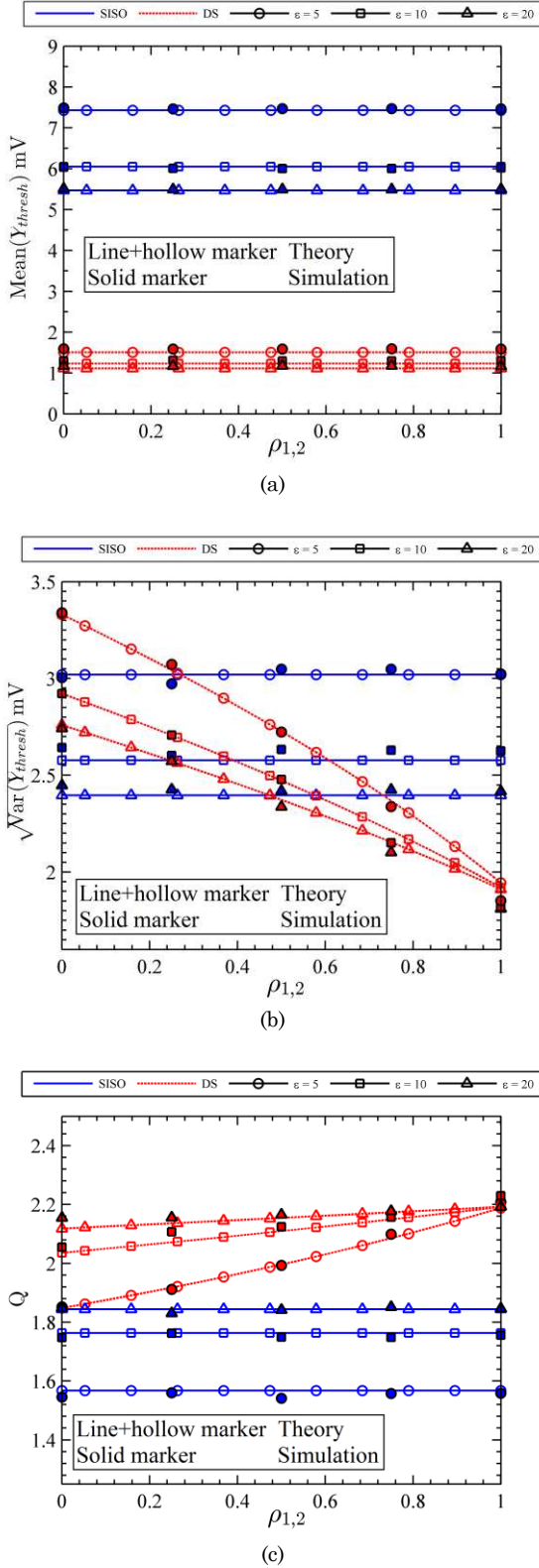
(a)

(b)

(c)

Fig. 4. Theory and simulation results for different ε_i over a range of correlation coefficient SNR of 12 dB and Rytov variance of 0.5: (a) mean of detection threshold $\mathrm{Mean}(Y_{thresh})$, (b) $\sqrt{\mathrm{Var}(Y_{thresh})}$ of detection threshold, and (c) Q-factor. SISO and DS refer to single-input single-output and differential signalling, respectively, while ε_i and $\rho_{1,2}$ denote extinction ratio and correlation coefficient, respectively.

and $\Phi_2 = 4.8$ mV. The value of $\rho_{1,2}$ spans from uncorrelated

(i.e., $\rho_{1,2} = 0$) to fully correlated channel conditions (i.e., $\rho_{1,2} = 1$). The accuracy of the proposed theory over the range of $\rho_{1,2}$ is obvious from the close agreement between simulated and predicted results as in Fig. 4.

For the differential signalling link, see Fig. 4(a), and case of $\Phi_1 \neq \Phi_2$ the values of $\mathrm{Mean}(Y_{TL})$ are almost the same (non-zero) and independent of $\rho_{1,2}$ for all values of ε, whereas $\sqrt{\mathrm{Var}(Y_{TL})}$ reduces with ε and $\rho_{1,2}$ reaching the minimum value of $\left(\sigma_{n,1}^2 + \sigma_{n,2}^2\right)^{1/2} = 1.9$ mV at $\rho_{1,2} = 1$, see Fig. 4(b). However, for the SISO link, as expected from (3a) and (5b) both $\mathrm{Mean}(Y_{TL})$ and $\mathrm{Var}(Y_{TL})$, respectively, are independent of $\rho_{1,2}$ and decrease with ε. This is because we kept the SNR at 12 dB and used a range of Φ_{SISO} for each given ε. Note that from (3a) $\mathrm{Mean}(Y_{TL})$ increases with Φ_{SISO}. Figure 4(c) illustrates the Q-factor as a function of $\rho_{1,2}$ for both differential signalling and SISO links based on (10). For the differential signalling link the Q-factor plot increases with $\rho_{1,2}$ reaching a maximum value of 2.2 at $\rho_{1,2} = 1$. For the SISO link the Q-factor plots are independent of $\rho_{1,2}$ increasing with ε_{SISO}. To summarize, if achievement of higher SNR is desirable in a differential signalling link then increasing ε_i would be the preferred option. However, one must also consider the optical source power vs. current characteristics to ensure linear operation to avoid non-linear induced distortions.

D. BER Performance

To validate our work, we will compare the predicted BER results from (16) with the simulated results for the same FSO system of the previous section. Figure 5 shows the predicted BER performance as the function of SNR for $\rho_{1,2}$ of 0 and 0.8 and C_n^2 of $1 \times 10^{-15} \mathrm{m}^{-2/3}$ and $2.5 \times 10^{-15} \mathrm{m}^{-2/3}$. The close agreement of the BER predicted from (16) with simulation results confirms the initial assumption of Y (i.e., the signal after subtraction) to be normal random variable for the case of differential signalling method.

As reported in [15] for fully correlated channels (i.e. $\rho_{1,2} = 1$) the turbulence has the minimum effect on the threshold level of the received signal, thus resulting in the same BER as in a clear channel. To investigate this, we have selected $C_n^2 = 5 \times 10^{-15} \mathrm{m}^{-2/3}$ and changed $\rho_{1,2}$ to 0, 0.5, 0.8, and 1 in Fig. 6, which illustrates the predicted and simulated BER as a function of the SNR for the differential signalling link. Figure 6 shows that the differential signalling link BER performance improves with $\rho_{1,2}$ as predicted in [15] and approaching the performance of a clear channel. For a BER of 10^{-4} the required SNR for a clear channel is $\sim$11.4 dB. From Fig. 6 we note that, for the same BER but different turbulence regimes the required power penalties are 4.6 dB, 2.6 dB, 1.1 dB, and 0 dB for $\rho_{1,2}$ of 0, 0.5, 0.8, and 1, respectively. Therefore, at high correlation values the performance of differential signalling is close to that of a clear channel.

V. EXPERIMENT

Based on the proposed scheme as shown in Fig. 1, we have developed an experimental setup to evaluate the link performance by generating uncorrelated (i.e., $\rho_{1,2} = 0$) and
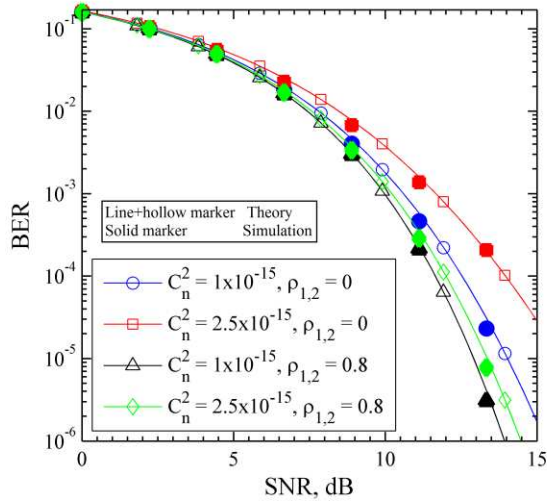
Fig. 5. BER versus SNR in dB of an FSO system implementing differential signalling method. Solid lines marked with small markers are based on the derived equations whilst large markers are obtained from the simulation. $\rho_{1,2}$ denotes correlation coefficient.
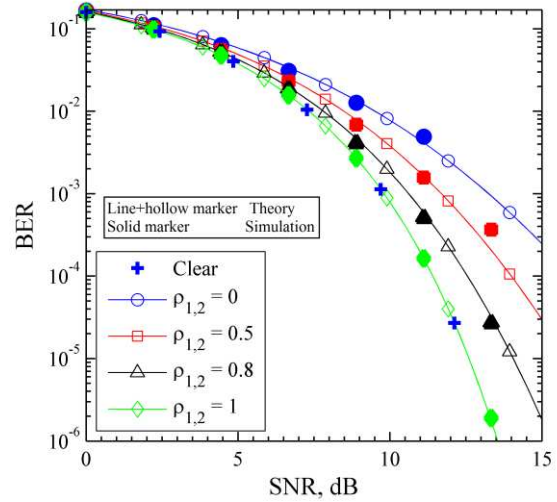

Fig. 6. BER versus SNR in dB of an FSO system implementing differential signalling method for $C_n^2 = 5 \times 10^{-15} \text{m}^{-2/3}$ and various correlation conditions. Solid lines with small markers are based on theory whereas large markers are obtained from simulation. The plus makers denote the clear channel condition. $\rho_{1,2}$ denotes correlation coefficient.

highly-correlated (i.e., $\rho_{1,2} \to 1$) channel conditions, see Fig. 7(a). Snapshots of the setup are also shown in Figs. 7(b,c). The laser beams from OSs (Figs. 7(a,b)) were launched into a 6 m-long laboratory turbulence chamber, which emulates an outdoor uncorrelated FSO turbulence channel (Figs. 7(a,c)). We denote the incident and reflected ray paths by PATH1 and PATH2, respectively (see Fig. 7(a)). In PATH1 OSs were spaced apart by a minimum distance of $d_r > 5$ mm to ensure uncorrelated fading conditions (i.e., $(d_r/\rho_0)^{5/3} > 5$). An adjustable mirror positioned at the other end of the chamber was used to increase the path length by reflecting the beams back towards the transmitting end. The reflected beams (i.e., PATH2 in Fig. 7(a)) were kept as close as possible to each other to ensure high correlation between the two paths. Heater fans were used to generate atmospheric turbulence within the chamber, see Fig. 7(a). To measure C_n^2, we have adopted the method of thermal structure parameter (based on the temperature gradient measurement) as in [28]. The temperature gradient was measured using 20 temperature sensors positioned along the chamber, see Fig 7(c). At the Rx end the reflected beams passed through a 50/50 beam splitter and were applied to two identical PIN PDs after optical filters, see Figs. 7(a,b). The outputs of PDs were captured using a real-time digital storage oscilloscope for further processing in MATLAB®.

We first investigated the effect of atmospheric turbulence on the uncorrelated path within the chamber. The reflected beams (i.e., PATH2) were passed through a pipe positioned within the chamber. The pipe ensured that beams propagating within did not experience any atmospheric turbulence, see Fig. 7(c). Similarly, we investigated the effect of atmospheric turbulence on the correlated path by isolating the uncorrelated channels (i.e., optical beams in PATH1 propagating through the pipe), see Fig. 3(a). Table II shows the entire key parameters adopted in the experiment.

Following the aforementioned approach, in this section

we present the measured Q-factor as well as for the differential signalling link with correlated and uncorrelated channel conditions for the SNR of ~24 dB as shown in Table III. Also included in Tnable III are C_n^2 and the equivalent σ_R^2 for λ_1 of 830 nm.

The peak to peak amplitude of individual signals were kept almost the same by adjusting the power of the modulating signal at the transmitter. In a clear channel the peak to peak amplitude of the differential signal at the Rx (i.e., $|\text{Mean}(Y_{\text{bit } 1}) - \text{Mean}(Y_{\text{bit } 0})|$) was directly measured to be ~410 mV and the standard deviation of the detection threshold $\sqrt{\text{Var}(Y_{\text{TL}})}$ was around 30 mV. We also assumed that, the variations in the signal levels representing bits 0 and 1, and the detection level are equally affected by turbulence (i.e., $\text{Var}(Y_{\text{bit } 0}) = \text{Var}(Y_{\text{bit } 1}) = \text{Var}(Y_{\text{TL}})$, therefore $\sqrt{\text{Var}(Y_{\text{bit } 1})} + \sqrt{\text{Var}(Y_{\text{bit } 0})} = 2\sqrt{\text{Var}(Y_{\text{TL}})} = 60$ mV. In this case, the Q-factor for the uncorrelated channel will be around 6, which is higher than the required Q-factor of 4.75 to achieve a BER of 10^{-6}.

To approximate the Q-factor in a correlated channel, we have assumed that $\text{Var}(y_1) \approx \text{Var}(y_2) = \text{Var}(Y)/2$. Then, by replacing $\text{Var}(y_1)$ and $\text{Var}(y_2)$ by $\text{Var}(Y)/2$ in the simplified version of detection threshold variance (i.e., $\text{Var}(Y_{\text{TL}}) = \text{Var}(y_1) + \text{Var}(y_1) - 2\rho_{1,2}\sqrt{\text{Var}(y_1)\text{Var}(y_2)}$), the approximate Q-factor for the correlated channel case is ~11. Note that the alternative solution would be the exact measurements of Φ_i, ε_i and $\rho_{1,2}$ and determination of the Q-factor using (9) and (10).

As was predicted in the previous section, the Q-factor is much higher for the correlated channel compared to the uncorrelated channel. Additionally, the measured value of $Q^2 \neq 10^{\text{SNR}/10}$, thus indicating no high correlation between channels. The measured $\rho_{1,2}$ was 0.7. As was outlined in [15] for longer FSO links, it is relatively simple to achieve high correlations between the channels and therefore to attain Q^2, which is much closer to $10^{\text{SNR}/10}$. Although the
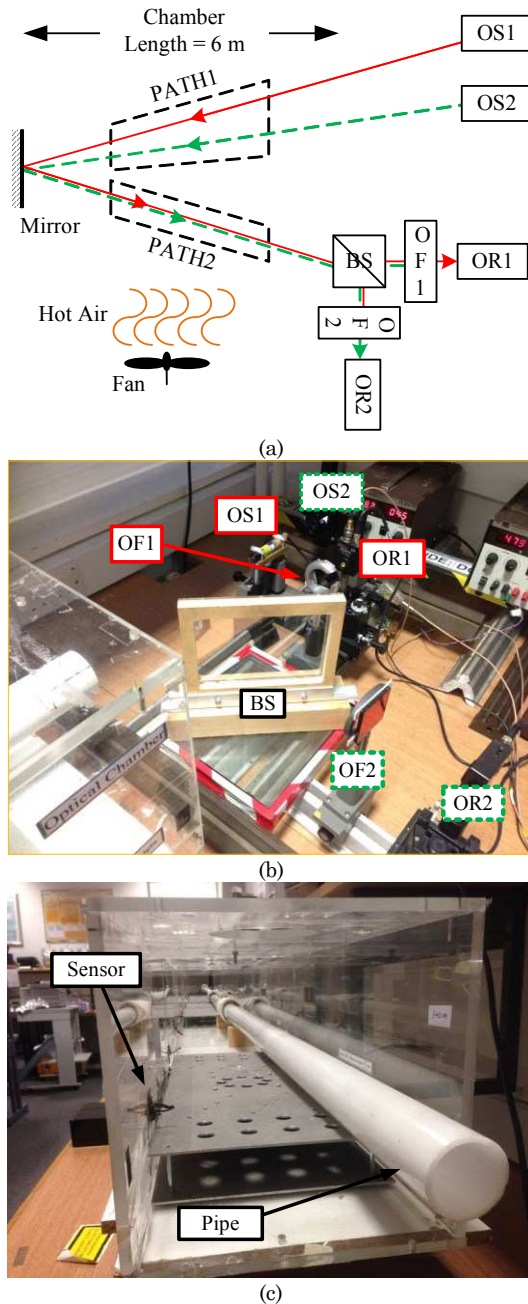
Fig. 7. Experimental setup: (a) schematic block diagram, (b) transmitters and Rx at one end of the chamber, and (c) atmospheric chamber with temperature sensors to measure temperature gradient, and a pipe to isolate either PATH1 or PATH2 from the turbulence conditions in the chamber. OS, BS, OF and OR refer to optical source, beam splitter, optical filter, optical RX, respectively.

TABLE II
THE DIFFERENTIAL SIGNALLING EXPERIMENTAL SETUP PARAMETERS

	Parameter	Value
	Data rate NRZ-OOK	100 kbps
	Chamber length L	6 m
Link 1	Optical transmit power	10 dBm
	Divergence angle	9.5 mDeg
	PD responsivity $\mathcal{R}_1$	0.3 A/W
	Wavelength λ_1	830 nm
Link 2	Optical transmit power	3 dBm
	Divergence angle	4.8 mDeg
	PD responsivity $\mathcal{R}_2$	0.4 A/W
	Wavelength λ_2	670 nm
	OR noise rms $\sqrt{\sigma_n^2}$	1.5 mV

and turbulence conditions are considered. For a BER of 10^{-6}, the SNR penalties are ~10 dB and ~2 dB for the SISO with turbulence and the differential signalling links (predicted and simulated), respectively compared to the SISO link with no turbulence.

Although the proposed differential signalling technique was validated especially for the case of an FSO link under the weak turbulence regime, it can be also adopted in the moderate and strong regimes. The expressions given in [29] and (4) can be used to determine the mean value and the variance of the detection threshold level under such conditions. For the case of the strong turbulence regime, the effect of beam wander should also be taken into consideration in addition to beam scintillation [8].

VI. CONCLUSION

The paper investigated the effects of link parameters as well as the channels' correlation coefficient on the detection threshold and the Q-factor of a differential signalling link with IM/DD NRZ-OOK. In this paper we at first derived

predicted results were based on the measured parameters, there is still a slight difference between the measured and predicted values. This difference is due to the fact that in the analytical approach the effect of noise was not considered and also for simplicity we assumed that the variations in the signal level (i.e., low and high levels representing bits 0 and 1, respectively) are the same as those of the detection threshold.

Figure 8 illustrates the predicted and simulated BER performance against the SNR for both differential signalling and SISO links for $\rho_{1,2} = 0.7$. For the SISO link both clear
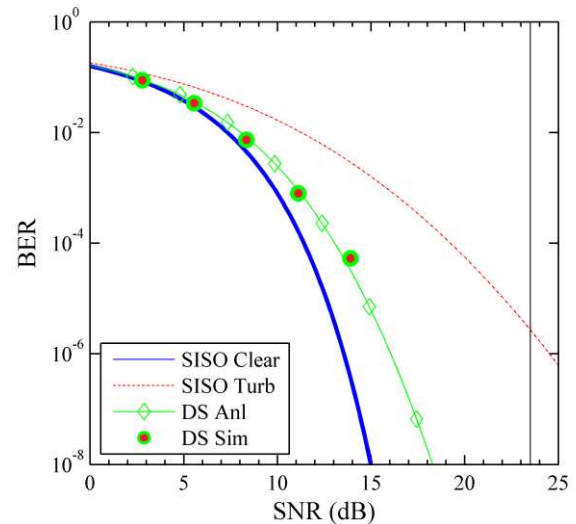

Fig. 8. BER versus SNR in dB of a SISO link in clear and turbulent conditions as well as DS link with a correlation coefficient of 0.7. The results are based on the theory and simulation.

TABLE III
THE SUMMERY OF THE EXPERIMENTAL MEASUREMENT FOR DIFFERENTIAL SIGNALLING (DS) LINK IN UNCORRELATED AND CORRELATED CONDITIONS. $\rho_{1,2}$, C_n^2, AND σ_R^2 DENOTE CORRELATION COEFFICIENT, THE REFRACTIVE INDEX STRUCTURE COEFFICIENT AND RYTOV VARIANCE, RESPECTIVELY.

Channels Condition	Measured Q	Predicted Q	$\rho_{1,2}$	C_n^2 (m$^{-2/3}$)	σ_R^2
Uncorrelated	6.32	6.95	0	5×10^{-11}	0.63
Correlated	10.13	11.14	0.7		

equations to describe the effect of weak turbulence on the received signal mean value, which can be used as a detection threshold level in a threshold decision-based receiver. We showed the significance of the link parameters as well as correlation coefficient on the threshold level. Also outlined was the analysis for the Q-factor of the received signal for the differential signalling link, showing improvement under correlated channels. We also showed that a system with a higher extinction ratio offered improved performance compared to a system with lower extinction ratio under the same SNR. Also derived was the closed-form expression for the BER for the differential signalling system under a weak turbulence regime. Results showed that for higher values of the correlation coefficient, the performance of the differential signalling system under turbulence approached that of a clear channel.

Finally, it was experimentally demonstrated that the Q-factor in a correlated channel is higher than the uncorrelated channel. The predicted and measured values of BER for SISO and differential signalling links were compared and it was shown that for lower SNR values differential signalling offered improved performance compared to SISO.

REFERENCES

[1] M. L. B. Riediger, R. Schober, and L. Lampe, "Decision-feedback detection for free-space optical communications," in *IEEE 66th Vehicular Technology Conference Fall. 2007*, 2007, pp. 1193-1197.

[2] S. Hitam, M. Abdullah, M. Mahdi, H. Harun, A. Sali, and M. Fauzi, "Impact of increasing threshold level on higher bit rate in free space optical communications," *Journal of Optical and Fiber Communications Research,* vol. 6, pp. 22-34, 2009/12/01 2009.

[3] Z. Ghassemlooy, S. Rajbhandari, and W. Popoola, *Optical wireless communications: system and channel modelling with MATLAB*. Boca Raton, FL: Taylor & Francis, 2013.

[4] M. A. Khalighi and M. Uysal, "Survey on free space optical communication: a communication theory perspective," *Communications Surveys & Tutorials, IEEE,* vol. 16, pp. 2231-2258, 2014.

[5] M. R. Bhatnagar and Z. Ghassemlooy, "Performance evaluation of FSO MIMO links in Gamma-Gamma fading with pointing errors," in *Communications (ICC), 2015 IEEE International Conference on*, 2015, pp. 5084-5090.

[6] Y. Fan, C. Julian, and T. A. Tsiftsis, "Free-space optical communication with nonzero boresight pointing errors," *Communications, IEEE Transactions on,* vol. 62, pp. 713-725, 2014.

[7] H. Hennes, D. Florian, G. Dirk, and C. Rapp, "Evaluation of FEC for the atmospheric optical IM/DD channel," in *Proc. SPIE: Free-Space Laser Communication Technologies XV*, 2003.

[8] L. C. Andrews and R. L. Phillips, *Laser beam propagation through random media*, Second Edition (SPIE Press Monograph Vol. PM152) ed.: SPIE Publications, 2005

[9] X. Zhu and J. M. Kahn, "Free-space optical communication through atmospheric turbulence channels," *Communications, IEEE Transactions on,* vol. 50, pp. 1293-1300, 2002.

[10] X. Zhu and J. M. Kahn, "Markov chain model in maximum-likelihood sequence detection for free-space optical communication through atmospheric turbulence channels," *Communications, IEEE Transactions on,* vol. 51, pp. 509-516, 2003.

[11] X. Zhu and J. M. Kahn, "Pilot-symbol assisted modulation for correlated turbulent free-space optical channels," in *Proc. SPIE 4489, Free-Space Laser Communication and Laser Imaging*, 2002, pp. 138-145.

[12] M. L. B. Riediger, R. Schober, and L. Lampe, "Fast multiple-symbol detection for free-space optical communications," *Communications, IEEE Transactions on,* vol. 57, pp. 1119-1128, 2009.

[13] M. L. B. Riediger, R. Schober, and L. Lampe, "Blind detection of on-off keying for free-space optical communications," in *Electrical and Computer Engineering, 2008. CCECE 2008. Canadian Conference on*, 2008, pp. 001361-001364.

[14] N. D. Chatzidiamantis, G. K. Karagiannidis, and M. Uysal, "Generalized maximum-likelihood sequence detection for photon-counting free space optical systems," *Communications, IEEE Transactions on,* vol. 58, pp. 3381-3385, 2010.

[15] M. Mansour Abadi, Z. Ghassemlooy, M. A. Khalighi, S. Zvanovec, and M. R. Bhatnagar, "FSO detection using differential signaling in outdoor correlated-channels condition," *Photonics Technology Letters, IEEE,* vol. 28, pp. 55-58, 2016.

[16] M. A. Khalighi, F. Xu, Y. Jaafar, and S. Bourennane, "Double-laser differential signaling for reducing the effect of background radiation in free-space optical systems," *Optical Communications and Networking, IEEE/OSA Journal of,* vol. 3, pp. 145-154, 2011.

[17] K. Prabu, D. S. Kumar, and T. Srinivas, "Performance analysis of FSO links under strong atmospheric turbulence conditions using various modulation schemes," *Optik - International Journal for Light and Electron Optics,* vol. 125, pp. 5573-5581, 2014.

[18] M. Mansour Abadi, Z. Ghassemlooy, M. R. Bhatnagar, S. Zvanovec, M. A. Khalighi, and A.-R. Maheri, "Using differential signalling to mitigate pointing errors effect in FSO communication link," in *IEEE International Conference on Commuinications ICC'16*, 2016.

[19] A. Leon-Garcia, *Probability and random processes for electrical engineering*. Reading, Mass: Addison-Wesley, 1989.

[20] S. M. Navidpour, M. Uysal, and M. Kavehrad, "BER performance of free-space optical transmission with spatial diversity," *Wireless Communications, IEEE Transactions on,* vol. 6, pp. 2813-2819, 2007.

[21] G. R. Osche, *Optical detection theory for laser applications*. New York: Wiley, 2002.

[22] M. A. Khalighi, N. Schwartz, N. Aitamer, and S. Bourennane, "Fading reduction by aperture averaging and spatial diversity in optical wireless systems," *Optical Communications and Networking, IEEE/OSA Journal of,* vol. 1, pp. 580-593, 2009.

[23] "G.976 : Test methods applicable to optical fibre submarine cable systems," ITU2010.

[24] A. A. Abu-Dayya and N. C. Beaulieu, "Comparison of methods of computing correlated lognormal sum distributions and outages for digital wireless applications," in *Vehicular Technology Conference, 1994 IEEE 44th*, 1994, pp. 175-179 vol.1.

[25]   M. S. Alouini and M. K. Simon, "Dual diversity over correlated log-normal fading channels," *Communications, IEEE Transactions on,* vol. 50, pp. 1946-1959, 2002.

[26]   M. Mansour Abadi, Z. Ghassemlooy, D. Smith, W. P. Ng, M. A. Khalighi, and S. Zvanovec, "Comparison of different combining methods for space-diversity FSO systems," in *Communication Systems, Networks & Digital Signal Processing (CSNDSP), 2014 9th International Symposium on*, 2014, pp. 1023-1028.

[27]   Z. Hajjarian, J. Fadlullah, and M. Kavehrad, "MIMO free space optical communications in turbid and turbulent atmosphere (Invited Paper)," *Journal of Communications,* vol. 4, pp. 524-532, 2009.

[28]   Z. Ghassemlooy, H. Le Minh, S. Rajbhandari, J. Perez, and M. Ijaz, "Performance analysis of ethernet/fast-ethernet free space optical communications in a controlled weak turbulence condition," *Lightwave Technology, Journal of,* vol. 30, pp. 2188-2194, 2012.

[29]   Y. Guowei, M. A. Khalighi, S. Bourennane, and Z. Ghassemlooy, "Approximation to the sum of two correlated Gamma-Gamma variates and its applications in free-space optical communications," *Wireless Communications Letters, IEEE,* vol. 1, pp. 621-624, 2012.